Pore occupancy changes water/ethanol separation in MOF -Quantitative map of coadsorption by IR

Mohamad El-Roz, Philippe Bazin, Tadeja Birsa Čelič, Nataša Zabukovec Logar, Frederic Thibault-Starzyk

Pore occupancy changes water/ethanol separation in MOF - Quantitative map of coadsorption by IR

Mohamad El-Roz,[a]‡ Philippe Bazin,[a]‡ Tadeja Birsa Čelič,[b] Nataša Zabukovec Logar,[b,c] Frederic Thibault-Starzyk[a]*

a) Laboratoire Catalyse et Spectrochimie, ENSICAEN, Université de Caen, CNRS, 6, boulevard du Maréchal juin, 14050 Caen, France

b) Laboratory for Inorganic Chemistry and Technology, National Institute of Chemistry, Hajdrihova 19, 1000 Ljubjana, Slovenia

c) University of Nova Gorica, Vipavska 13, 5000 Nova Gorica, Slovenia

KEYWORDS: FTIR spectroscopy, in-situ gravimetry, MIL-100(Fe), water-ethanol separation.

Abstract

The conventional distillation method to separate ethanol from water is energy-intensive and inefficient due to the presence of the azeotropic point of the binary system. Various processes have been proposed as potential separation techniques. Among them, preferential adsorption-based separation is considered to be an efficient and energy-saving method for purification due to the easy regeneration under relatively mild conditions. In this work, the co-adsorption of gaseous water and ethanol on porous metal-organic framework (MIL-100(Fe)) in various

proportions has been studied by coupling FTIR spectroscopy with in-situ gravimetry (AGIR). The quantifications of co-adsorbed water and ethanol on the MIL-100(Fe) have been performed under different conditions (P/P0). Ethanol is preferentially adsorbed on MIL-100(Fe). Vapor-liquid equilibrium of water/ethanol was altered when the pore volume of the MIL-100(Fe) was partially occupied. Our results suggest that the optimal conditions for the separation of H2O/EtOH on MIL-100(Fe) is at EtOH(P/Po)<0.05 with H2O(P/Po)<0.4 at room temperature.

Introduction

Separation of ethanol/water mixture is of great significance because the ethanol use as alternative to oil-based fuels and as a fuel additive.[1,2] The recent push for ethanol as an additive to gasoline has motivated the research interests in the production of anhydrous ethanol.[3,4] In fact, water is always present in ethanol produced from the fermentation of biomass, and it is also found in ethanol produced via the catalytic hydration of ethylene. The conventional distillation method to separate ethanol from water is energy-intensive and inefficient due to the presence of the azeotropic point of the binary system (azeotrope at an 89.4:10.6 molar ratio, 78.2°C, and 1 atm of pressure),[5] and only about 4 wt.% of water could be removed from ethanol by distillation. To circumvent these problems, various processes including liquid–liquid extraction, pervaporation, and adsorption in porous materials and molecule sieves have been proposed as potential separation techniques.[6] Among them, preferential adsorption-based separation is considered to be an efficient and energy-saving method for purification due to the easy regeneration under relatively mild conditions.[7,8]

Compared with traditional porous sorbents such as activated carbons and inorganic zeolites, metal organic frameworks (MOFs) materials have advantages for specific adsorption and separation. MOFs that are formed via coordination between metal centers and organic linkers possess extremely large surface areas and well-defined pores. They are predicted to be highly efficient for many potential applications in gas-separation membranes,[9] selective gas adsorption,[10] hydrogen[11] and CO_2[12-14] storages, catalysis,[15] and sensing.[16] Diverse interactions between host frameworks and guest molecules, such as hydrogen-bonding, π-stacking, and van der Waals interactions, can be engaged to affect the selectivity and performance of adsorption.[17] To date, progress has been made in the construction of porous framework materials with selective adsorption towards alcohols or water,[18-22] but the practical separation of alcohol/water mixtures, which is more complicated than single-component adsorption experiments, has rarely been explored.[23] Based on density functional theory study, a combination of hydrogen bonding between the hydroxyl group in ethanol and MOF framework as well as van der Waals interactions between the ethanol alkyl chain with the phenyl ring in MOF were determined to be crucial for the alcohol-water separation in Zn-based MOF.[8] In another computational study, the alterations of H-bond network together with water-alcohol separation were attributed to confiment effects in the silicalite-1 environment.[24]

In this paper, our work is focused on the preferential adsorption on MIL-100(Fe) from gas water–ethanol mixtures. A new and successful approach has been used. It is based on the coupling infrared spectroscopy and in-situ gravimetry (AGIR). IR spectroscopy is a powerful and recognized technique to study the adsorbed species present on material surfaces (silica, zeolites, mesoporous materials, etc.). It allows one to quantify the adsorbates, e.g. water, and to characterize the active sites.[25] In-situ gravimetry permits to determine the mass adsorbed under

different relative pressures. Therefore, a coupling of transmission IR spectroscopy with in-situ gravimetry is essential to determine the molar absorbance coefficients for the characteristic vibration bands of adsorbates, such as water and ethanol. Consequently, the quantification of water and ethanol co-adsorbed on the surface from different vapor water/ethanol mixtures and/or under different conditions becomes possible. Such a study allows highlighting the material performance not only for water/ethanol separation, but it also opens the way to study the adsorption of vapor mixtures on porous materials.

Experimental Section

Synthesis and characterization

An iron-based MOF material MIL-100(Fe) was synthesized hydrothermally from commercially available reagents. The final single crystalline phase was obtained after crystallization in Teflon-lined autoclaves at 150 °C (5 days) from a mixture of reagents in following molar ratio: 3 $FeCl_3 \cdot 6H_2O$ (98 %, Aldrich) : 1 $C_9H_6O_6$ (95 %, Aldrich) : 80 H_2O (deionized in-house) : 2 NaOH (pro analysi, Merck) without the use of hydrofluoric acid or any other mineralizing agent commonly needed for a successful synthesis. [26] The as-synthesized material was activated by stirring in deionized water under reflux at 100 °C for 16 h. Finally, the activated orange powder of MIL-100(Fe) material was filtered off and dried in air at room temperature. The crystal structure and phase purity were confirmed by matching measured and calculated X-ray diffraction patterns. In our previously published work we already explained that, most probably, one fluorine atom per trimer, which is usually present in the structure of MIL-100 materials, is in our structure replaced by OH group since MIL-100(Fe) material was prepared without the use of HF. The MIL-100(Fe) morphology of octahedraly shaped crystals was confirmed with a

scanning electron microscope Zeiss Supra™ 3VP and elemental analyses results are consistent with the stoichiometry of MIL-100(Fe) final material (weight %): Fe, 18.2 (calc. 19.6); C, 27.3 (calc. 25.2); H, 3.9 (calc. 4.0). EDX analysis was performed on a SUPRA 35 VP (Carl Zeiss) scanning microscope equipped with a spectrometer Inca 400 (Oxford Instruments), C, H, N, S analyses were obtained once Perkin-Elmer CHNS Elemental Analyzer. MIL-100(Fe) thermal stability was checked by thermogravimetric analysis on METTLER TOLEDO TGA/SDTA (measurements were carried out in an air flow with a heating rate of 10 K/min from 25 °C to 800 °C) and textural properties were evaluated from N_2 adsorption isotherms measured at 77 K on a Micromeritics 2020 volumetric adsorption analyzer. The isotherm shows type-I curves, the BET surface area is 1136 m^2g^{-1} (p/p^0 = from 0.01 to 0.12) and the micropore volume estimated by the Dubinin-Astakhov equation is 0.38 $cm^3 \cdot g^{-1}$, which is comparable with previously reported data.[26-28] Additionally, the hydrothermal stability of MIL-100(Fe) material was tested by boiling in distilled water for different periods of time up to 24 hours under reflux. The structure did not change in water at ambient temperature not in boiling water for at least 24 hours, therefore the structure is very stable in water media.

AGIR technique

This technique developed recently in our laboratory allows measuring simultaneously the weight and IR spectra of a solid sample under gas flow, between room temperature and 773 K. The setup has been described in detail by Bazin et al. [[29]] and has showed its interest in several works related to the quantification of adsorbed species on different materials.[29-32] In this work, the AGIR was used to evaluate both water and ethanol adsorbed on MIL-100(Fe) sample at room temperature, versus the partial pressures water-ethanol vapor mixture. Analyses were carried out

on self-supported pellets (2 cm² - 20 mg). Infrared spectra of the sample were recorded with a Nicolet 6700 spectrometer equipped with a MCT detector (64 scans / 4 cm^{-1} resolution) within a broad spectral range [6000 – 600 cm^{-1}]. The infrared spectra and mass changes of the sample, for each H_2O/C_2H_5OH mixture investigated, were recorded after reaching the equilibrium, as indicated by the absence of change in the sample mass and infrared spectra. Additional indication for the occurrence of equilibrium was provided by a MS analyzer (Pfeiffer Omnistar GSD301), which was used for the monitoring of H_2O/C_2H_5OH concentrations in the Ar outlet flow.

Results

The porosity of MIL-100(Fe) originates from both 25 Å and 29 Å mesopores, which are accessible via 5.5 Å and 8.6 Å windows, respectively.[26] MIL-100(Fe) mesopores are easily accessible toward water and ethanol via the both windows, with a water and ethanol kinetic diameters equal to 2.68 Å and 4.5 Å, respectively. Therefore, the preferential water or ethanol adsorption depends of the interaction forces between these molecules and the MIL-100(Fe) surface.

Water and Ethanol isotherms on MIL-100(Fe)

Figure 1 shows the IR spectra of MIL-100(Fe) after water and ethanol (EtOH) adsorption, at room temperature (RT), in the region of H_2O and C-C-O vibrations. Water can be easily distinguished using the combination band ($\nu_2 + \nu_3$) of molecular water, at 5210 cm^{-1}, hereafter called $(\nu+\delta)H_2O$. The characteristic $(\delta)H_2O$ vibration band centered at around 1635 cm^{-1} could not be easily observed in our case due to the saturation of this region by the IR absorption of the benzoate ligand in the MIL-100(Fe) structure. The new bands observed after ethanol adsorption

at 1092 cm^{-1}, 1041 cm^{-1} and 877 cm^{-1} are assigned to the C-O stretching vibration, and to the asymmetric and symmetric stretching vibrations of C-C-O, respectively.[33] The 877 cm^{-1} band is selected to quantify the adsorbed ethanol owing to its relatively low absorption coefficient (no saturation at high ethanol concentrations) without overlap with the dry or wet MIL-100(Fe) structure vibrations.

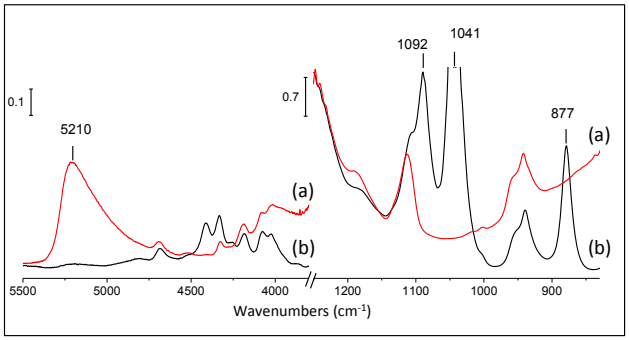

Figure 1. IR spectra of MIL-100(Fe), in the region of H_2O and C-C-O vibrations, after water (a) and ethanol (b) adsorption, at RT.

The vapor adsorption studies were carried out using AGIR technique under atmospheric pressure and at room temperature. Water and ethanol adsorption isotherms give a valuable first estimate of the adsorption behavior and allow calculating the molar absorption coefficients of the characteristic vibration bands of water and ethanol. **Figure 2** shows the rise of the intensities of the characteristic vibration bands of water and ethanol, adsorbed on MIL-100(Fe), with the increase of the relative pressures of water (**Figure 2-A**) or ethanol (**Figure 2-B**), respectively. Therefore, optical isotherms of water and ethanol on MIL-100(Fe) are obtained by integration of the IR bands at 5210 cm^{-1} and at 877 cm^{-1} (**Figures 3A-I and 3B-I**), respectively. The water isotherm is in good agreement with results previously published for MIL-100(Fe).[34] At small

relative pressures (p/p_o<0.15), a first adsorption and cluster formation of water at the hydrophilic metal sites take place.[35] The steep rise at 0.15<p/p_o<0.50 has been soundly explained by the consecutive filling of, first, the 25 Å mesopores, then of the 29 Å mesopores. For ethanol, a type I isotherm is obtained.

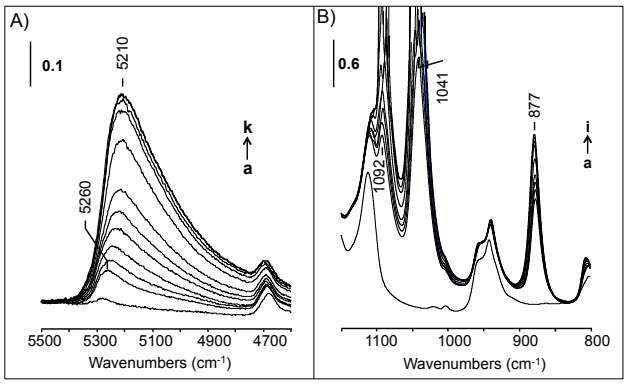

Figure 2. Evolution of IR spectra of MIL-100 (Fe) after water (A) and ethanol (B) adsorption at different relative pressures (P/P_o): a) 0.000, b) 0.016, c) 0.048, d) 0.100, e) 0.200, f) 0.300, g) 0.400, h) 0.500, i) 0.600, j) 0.800, k) 0.900. IR spectra were collected after 1h of stabilization at the corresponding P/P_o. (Ar was used as carrier gas with 25 cm^3/min total flow at RT; $m_{MIL-100(Fe)}$=20 mg).

On the other hand, the in-situ gravimetry analysis shows the evolutions of mass gains (adsorbed mass) of MIL-100(Fe) during ethanol and water adsorptions (**Figure S1**). The adsorption isotherms and the optical isotherms have a totally similar shape. The Langmuir simulation of

these isotherms provide total pore volume around 0.39 ± 0.02 $cm^3.g^{-1}$ and 0.35 ± 0.02 $cm^3.g^{-1}$, estimated from ethanol and water gravimetric adsorption isotherms (using the specific volumic mass parameters), respectively (**Figure S2**). These values are in agreement with those obtained from the N_2-adsorption isotherm (0.38 cm^3/g), confirming a full pore accessibility of MIL-100(Fe) toward water and ethanol.

Based on the optical and gravimetric isotherms of pure water and pure ethanol, the molar absorption coefficients of the vibration bands at 5210 cm^{-1} and 877 cm^{-1} were then determined. They were calculated from the relationship between the areas of the characteristic vibration bands of the adsorbates and their corresponding amounts (**Figure 3**). According to the Beer-Lamber law (**equations 1**), they are equals to the slopes of the curves for the IR band area evolution versus the corresponding amount of adsorbed molecules, taking into account the geometric area of the MIL-100(Fe) pellet. Consequently, the molar absorbance coefficient for $(\nu+\delta)H_2O$ and for $(\nu_{as})C\text{-}C\text{-}O$ (of ethanol), adsorbed on MIL-100(Fe), are found to be equal to 0.796 ± 5 10^{-3} $cm.\mu mol^{-1}$ and 0.726 ± 5 10^{-3} $cm.\mu mol^{-1}$, respectively.

$$\mathbf{A_\nu = \varepsilon_\nu.l.C = \varepsilon_\nu.l.n/V = \varepsilon_\nu.l.n/(s.l) = \varepsilon_\nu.n/s} \qquad \text{(equation 1)}$$

With:

A (cm^{-1}): IR band area of the band situated at ν-wavenumber;

ε ($\mu mol^{-1}.cm$) $_\nu$: corresponding molar absorption coefficient;

l (cm) : optical pathway (pellet thickness);

n (μmol) : molar number of the adsorbent;

s (cm^2) : MIL-100(Fe) pellet surface (2 cm^2).

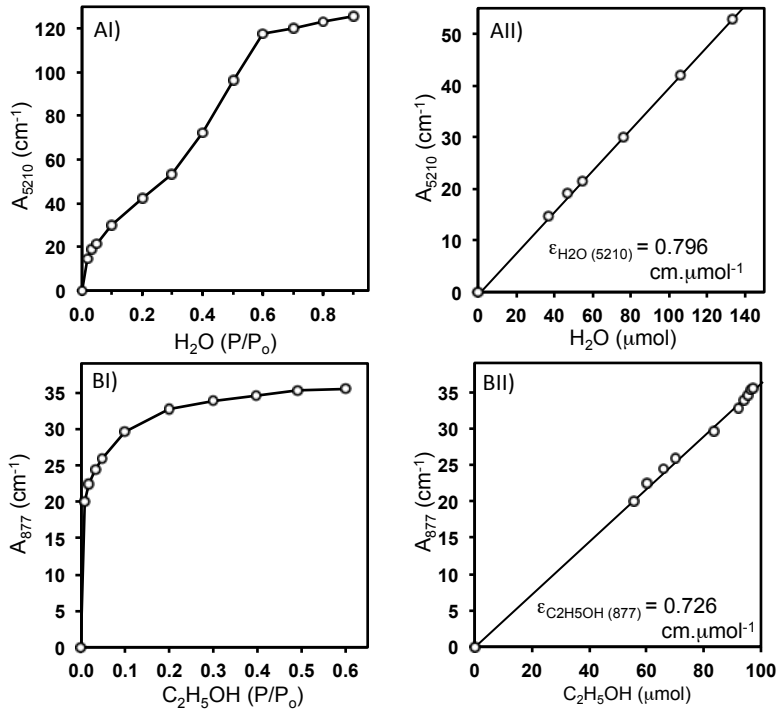

Figure 3. Optical adsorption isotherms of water (AI) and ethanol (BI) on MIL-100(Fe) at RT using the band area (A_ν) of the characteristic vibration bands of water ($\nu+\delta$ H_2O) and ethanol (ν_{as} C-C-O) at 5210 cm^{-1} and 877 cm^{-1}, respectively. Figures (AII) and (BII) represent the evolution of A_ν versus the amounts of water (AII) and ethanol (BII) adsorbed on MIL-100(Fe) (these amounts are determined from the in-situ gravimetry analysis Figure S-1). The slopes of the line

trend correspond to the molar absorption coefficient values of the corresponding IR bands (insert AII and BII).

Based on these results, the amounts of water and ethanol, co-adsorbed on MIL-100(Fe) from a water/ethanol vapor mixture, are then determined from the IR absorbance at 5210 cm^{-1} and 877 cm^{-1}, respectively (**equation 2**):

$$\mathbf{N}(mmol/g) = \frac{\mathbf{A}(cm^{-1}) * \mathbf{s}(cm^2)}{\varepsilon_{\nu}(\mu mol^{-1}.cm) * \mathbf{m}(mg)}$$

(equation 2)

With:

N: molar number of adsorbed water or ethanol per gram of MIL-100(Fe) (=n/m);

m: mass of the MIL-100(Fe) pellet.

Water/ethanol vapor mixture isotherms on MIL-100(Fe)

Figure 4 displays the mass gains on a MIL-100(Fe) pellet during adsorption from various water/ethanol vapor mixtures, as a function of the relative pressures of ethanol (A) and water (B). No significant change is noted at relatively high water vapor pressure (P/Po>0.1). On the other side, the presence of ethanol in the gas phase, even in low concentration, changes drastically the adsorption isotherm of water (**Figure 4-B**). Without direct qualitative information on the species adsorbed on MIL-100(Fe), the interpretation of these gravimetric results is impossible. This explains our choice of AGIR as a technique to perform this complicate study by coupling information on the surface (transmission IR) with gravimetry.

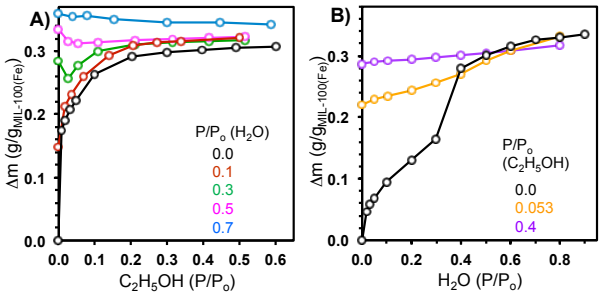

Figure 4. Evolution of the mass gain of MIL-100(Fe) versus ethanol (P/P_o) with different relative pressures of water (A) and versus water (P/P_o) with different relative pressures of ethanol (B). T=300 k; stabilizing time at each P/P_o=1h.

The analysis of the IR spectra of MIL-100(Fe) collected under the previous conditions shows variations in the amount of water and ethanol co-adsorbed on MIL-100(Fe) under different conditions (**Figure S3**). The optical isotherms of water and ethanol for various water/ethanol vapor mixtures are calculated according to the **equation 2** and are reported in **Figure 5**. It is clear that the presence of water together with ethanol in the gas phase results in a modification in the original adsorption isotherms of absolute ethanol or pure water. This is assigned to an adsorption competition between ethanol and water on MIL-100(Fe) and related to various thermodynamic factors such as the relative pressures of the molecules, and to the different interactions between the adsorbates and MIL-100(Fe) surface. The effect of water on ethanol adsorption isotherms is presented in **Figure 5-A**. The increase of the water vapor pressure

decreases the total amount of adsorbed ethanol. The effect is more pronounced at relatively high water concentration. These results demonstrate that even if is no significant change in the mass (eg. **Figure 4A** for $H_2O(P/P_o=0.7)$), the adsorbed water/ethanol ratios on MIL-100(Fe) could be completely different (**Figures 5 A-I A-II**), depending of $EtOH(P/P_o)$ and $H_2O(P/P_o)$. The effect of ethanol on water adsorption isotherms is much more important. The presence of ethanol in the gas phase (even at relatively low concentration; $P/P_o=0.053$) changes the water adsorption isotherm from type IV to a type V isotherm (**Figure 5-B-II**). These results assigned to a preferential adsorption of ethanol on MIL-100(Fe).

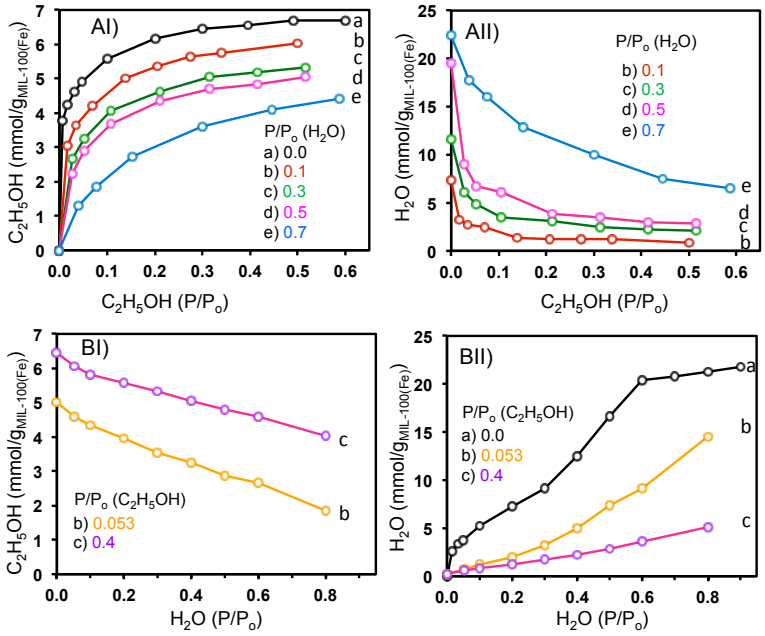

Figure 5. Evolution of adsorbed ethanol (A-I and B-I) and water (A-II and B-II) amounts (in mmol/g) on MIL-100(Fe) versus $EtOH(P/P_o)$ in presence of water (with $(P/P_o)_{water}$=0.0; 0.1; 0.3; 0.5; 0.7) (A) and versus

$H_2O(P/P_o)$ in presence of ethanol (with $(P/P_o)_{ethanol}$=0.0; 0.053; 0.04) (B). T=300 K; Total flow (Ar)= 25 cm^3/min.

In order to explore the preferential adsorption of ethanol on MIL-100(Fe), a 2D cartography of the amounts of adsorbed water and ethanol versus (P/P_o) is presented in **Figure 6**. The values, collected from the various experiments realized under different ethanol/water vapor ratios, allow estimating the amount of co-adsorbed water and ethanol on MIL-100(Fe). **Figure 6** reveals that ethanol is preferentially adsorbed on MIL-100(Fe) for a $0.0<H_2O(P/P_o)<0.4$, and for $H_2O(P/P_o)>0.4$ with $EtOH(P/P_o)>0.35$. But these results could not exclude totally the adsorption of water (even in small amount) on MIL-100(Fe). We think that water is adsorbed (chemisorbed) on the Fe metal sites of MIL-100(Fe) but this adsorption become negligible compared to the adsorption of ethanol on the MOF surface.

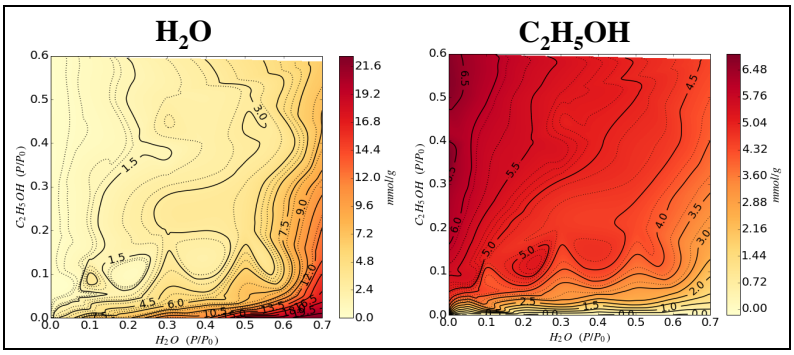

Figure 6. 2D cartography of the adsorbed water and ethanol evolution on MIL-100(Fe) versus (P/P_o) of ethanol and water. A preferential ethanol adsorption is observed even at low ethanol partial pressures.

Evolution of the occupation of the MIL-100(Fe) porosities versus (P/P_0) of water and ethanol is presented **Figure 7**. The volumes occupied by ethanol and water have been estimated using the density of these molecules at RT (0.789 g/cm^3 and 1.00 g/cm^3 respectively) and water/ethanol amounts (determined as detailed above). The result shows that the porosity of the MIL-100(Fe) is completely full for $H_2O(P/P_o)>0.4$ with $EtOH(P/P_o)>0.05$. These results are then used in order to highlight the optimal conditions for a preferential adsorption of ethanol on MIL-100(Fe).

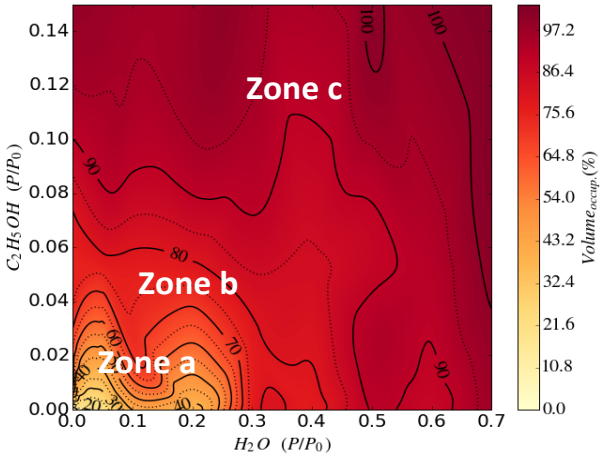

Figure 7. Evolution of the pore volume occupation (in %) by water/ethanol mixture versus (P/P_o) of ethanol and water. Zones a, and c correspond to a partial (0.0-60.0%), high (80.0-100.0%) and fully occupied porous volume of MIL-100(Fe) with water/ethanol).

Preferential adsorption of ethanol on MIL-100(Fe)

The evolution of the fraction of adsorbed ethanol versus vapor ethanol fraction for ethanol-water binary mixtures is presented in **Figure 8**. The values are distributed in three main regions: a, b and c. These regions correspond to the zone a, zone b and zone c in **Figure 7**. In the region

corresponding to a total pore occupation (zone c) the trend line follows the traditional vapor-liquid equilibrium of the water-ethanol binary mixtures at room temperature.[36] Therefore, in this region, the adsorbent (MIL100(Fe) has no significant effect. Vapor-liquid equilibrium is altered for partial pore occupations (a and b zones in **Figure 8**) showing the role of the MIL-100(Fe) surface in the preferential adsorption of ethanol. This variation can be assigned to the intermolecular interactions between the (phenyl) and oxy functions of the MIL-100(Fe) ligands with the ethyl and alcohol functions of the ethanol, respectively. In other hand, presence of water (in low concentration) could lead to the formation of new acid sites by the chemisorption of water clusters on the metal centres.[35] These sites promote then the ethanol adsorption via hydrogen bonding with the alcohol function (the pK_b of ethanol is higher than that of water). Thus, at the interface between liquid and solid, the adjacent layers of dissimilar molecules are in force fields very different from those existing in the bulk liquid. Moreover, these long-range interactions would affect not only the molecular cohesive forces in the liquid phase but also the interfacial surface energy, and thus altering the vapor-liquid equilibrium (VLE) of the binary mixture. When the MIL-100(Fe) pores are almost occupied, the liquid-liquid interaction become dominant and the effect of the support on the bulk liquid (present on the pore) is insignificant. To conclude, these result indicate that the optimal condition for the separation of water/alcohols on MIL-100(Fe) is for EtOH(P/P_o)<0.05 and H_2O(P/P_o)<0.4 (zone a in **Figure 8**).

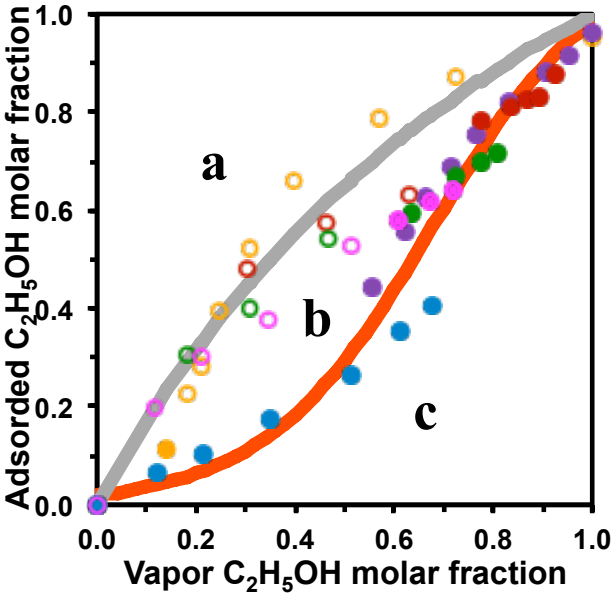

Figure 8. Evolution of the adsorbed ethanol molar fraction versus the vapor ethanol molar fraction. Open and close symbols correspond to the ethanol amounts for partial and total mesopores occupations, respectively. Red line (zone c) corresponds to the liquid-vapor equilibrium of ethanol from ethanol-water binary system at RT (Ref. 36). Grey line (zone a) corresponds to the competitive Langmuir adsorption isotherm simulation with k_{H2O}=0.914 10^{-3} and k_{C2H5OH}=1.692 10^{-3}. The a, b and c zones correspond to a 0-80%,

80-100% and 100% relative pore volume occupation by ethanol and/or water.

Conclusion

In this work we have studied the preferential adsorption of water or ethanol from gas water–ethanol mixtures on MIL-100(Fe) by coupling in-situ gravimetry with infrared spectroscopy (AGIR). Coupling the transmission IR spectroscopy with in-situ gravimetry (AGIR) allowed determining molar absorbance coefficients for the characteristic vibration bands of water (at 5210 cm^{-1}) and ethanol (at 877 cm^{-1}). They were found to be equal to 0.796 $cm.\mu mol^{-1}$ and 0.726 $cm.\mu mol^{-1}$, respectively. Then, the quantification of water and ethanol co-adsorbed on the surface from different vapor water/ethanol mixtures was realized using this new approach. We have shown that ethanol is preferentially adsorbed on MIL-100(Fe) for $0.0<H_2O(P/P_o)<0.4$ with $0.0<EtOH(P/P_o)<1.0$, or for $H_2O(P/P_o)>0.4$ with $EtOH(P/P_o)>0.35$. The experimental results demonstrate that the vapor-liquid equilibrium of water-ethanol binary mixtures is altered when the pore volume of MIL-100(Fe) is partially occupied (for $EtOH(P/P_o)<0.05$ and $H_2O(P/P_o)<0.4$). The approach (AGIR) proposed in this work is very promising to future studies of the co-adsorption of water ethanol on different types of porous materials.

ASSOCIATED CONTENT

Supporting Information. Evolution of the mass gain of MIL-100(Fe) during water (A) and ethanol (B) adsorption on MIL-100 (Fe) at 300 k. Estimation of the occupied micropores of MIL-100(Fe) by water and ethanol using Langmuir model. Evolution of the IR spectra of MIL-100 (Fe), in the region of $(\nu+\delta)H_2O$ and (ν) C-C for various partial pressure of water/ethanol mixtures. This material is available free of charge via the Internet at http://pubs.acs.org.

AUTHOR INFORMATION

Corresponding Author

E-mail: mohamad.elroz@ensicaen.fr
Fax: 0033 2 31 46 2732

Author Contributions

‡These authors contributed equally.

Table of Contents

New approach based on the coupling of FTIR spectroscopy with gravimetry has been used to study the co-adsorption of water and ethanol from water/ethanol mixtures on MIL-100(Fe). A preferential adsorption of ethanol was observed. The vapor-liquid equilibrium of water-ethanol binary mixtures is altered when the pore volume of MIL-100(Fe) is partially occupied (optimal condition for water/ethanol separation).

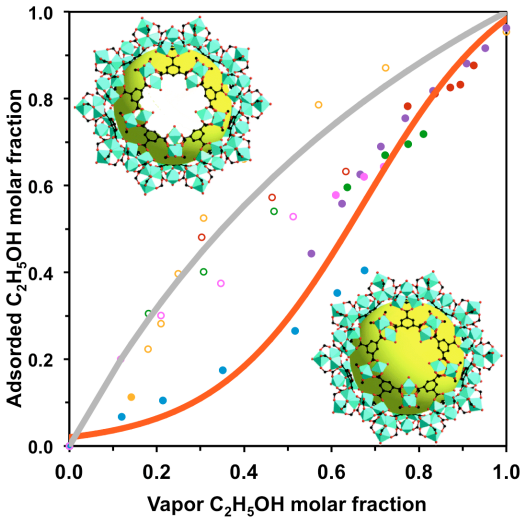

REFERENCES

[1] Hill, J. ; Nelson, E. ; Tilman, D. ; Polasky, S. ; Tiffany, D. Environmental, economic, and energetic costs and benefits of biodiesel and ethanol biofuels *Proc. Natl. Acad. Sci.* **2006**, *103*, 11206-11210.

[2] Lively, R. P. ; Dose, M. E. ; Thompson, J. A. ; McCool, B. A. ; Chance, R. R. ; Koros, W. J. Ethanol and water adsorption in methanol-derived ZIF-71, *Chem. Commun.* **2011**, *47*, 8667-8669.

[3] Chum, H. L. ; Overend, R. P. Biomass and renewable fuels. *Fuel Process Technol*. **2001**, *71*, 187-195.

[4] Goldemberg**,** J. Ethanol for a Sustainable Energy Future, *Science* **2007**, *315*, 808-810.

[5] Treybal, R.E. *Mass-transfer operations, 3rd ed.,* McGraw-Hill Book Co. Singapore,**1980**.

[6] Kumar, S.; Singh, N.; Prasad, R. Anhydrous ethanol: a renewable resource of energy, *Renew. Sust. En. Rev.* **2010**, *14*, 1830-1844.

[7] Phan, A. ; Cole, D. R. Striolo, ; A. Preferential Adsorption from Liquid Water–Ethanol Mixtures in Alumina Pores, *Langmuir* **2014**, *30*, 8066-8077.

[8] Wang, C. H. ; Bai, P. ; Siepmann, J. I. ; Clark, A. E. Deconstructing Hydrogen-Bond Networks in Confined Nanoporous Materials: Implications for Alcohol–Water Separation, *J. Phys. Chem. C*, **2014**, *118*, 19723-19732.

[9] Haldoupis, E. ; Nair, S. ; Sholl, D. S. Efficient Calculation of Diffusion Limitations in Metal Organic Framework Materials: A Tool for Identifying Materials for Kinetic Separations, *J. Am. Chem. Soc.* **2010**, *132*, 7528-7539.

[10] Li, J. R.; Kuppler, R. J.; Zhou, H. C. Selective gas adsorption and separation in metal–organic frameworks, *Chem. Soc. Rev.* **2009**, *38*, 1477-1504.

[11] Murray, L. J. ; Dinca, M. ; Long, J. R. Hydrogen storage in metal–organic frameworks, *Chem. Soc. Rev.* **2009**, *38*, 1294-1314.

[12] Millward, A. R. ; Yaghi, O. M. Metal−Organic Frameworks with Exceptionally High Capacity for Storage of Carbon Dioxide at Room Temperature, *J. Am. Chem. Soc.* **2005***, 127,* 17998-17999.

[13] Soubeyrand-Lenoir, E. ; Vagner, C. ; Yoon, J. W. ; Bazin, P. ; Ragon, F. ; Hwang, Y. K. ; Serre, C. ; Chang, J.-S. ; Llewellyn, P. L. How Water Fosters a Remarkable 5-Fold Increase in Low-Pressure CO_2 Uptake within Mesoporous MIL-100(Fe) *J. Am. Chem. Soc.* **2012**, *134*, 10174-10181.

[14] Leclerc, H. ; Vimont, A. ; Lavalley, J.-C. ; Daturi, M. ; Wiersum, A. D. ; Llwellyn, P. L. ; Horcajada, P. ; Férey, G. ; Serre, C. Infrared study of the influence of reducible iron(III) metal sites on the adsorption of CO, CO_2, propane, propene and propyne in the mesoporous metal–organic framework MIL-100, *Phys. Chem. Chem. Phys.* **2011**, *13*, 11748-11756.

[15] Lee, J.; Farha, O. K.; Roberts, J.; Scheidt, K. A.; Nguyen, S. T.; Hupp, J. T. Metal–organic framework materials as catalysts, *Chem. Soc. Rev.* **2009**, *38*, 1450-1459.

[16] Zacher, D. ; Shekhah, O. ; Woll, C. ; Fischer, R. A. Thin films of metal–organic frameworks *Chem. Soc. Rev.* **2009**, *38*, 1418-1429.

[17] Serre, C. ; Mellot-Draznieks, C. ; Surblé, S. ; Audebrand, N. ; Filinchuk, Y. ; Férey, G. Role of Solvent-Host Interactions That Lead to Very Large Swelling of Hybrid Frameworks, *Science* **2007**, *315*, 1828-1831.

[18] Lively, R. P. ; Dose, M. E. ; Thompson, J. A. ; McCool, B. A. ; Chance, R. R. ; Koros, W. J. Ethanol and water adsorption in methanol-derived ZIF-71, *Chem. Commun.* **2011**, *47*, 8667-8669.

[19] Zhang, K. ; Zhang, L. ; Jiang, J. **2013**, Adsorption of C1–C4 Alcohols in Zeolitic Imidazolate Framework-8: Effects of Force Fields, Atomic Charges, and Framework Flexibility, J. Phys. Chem. C *117*, 25628-635.

[20] Borjigin, T. ; Sun, F. X. ; Zhang, J. L. ; Cai, K. ; Ren, H. ; Zhu, G. S. microporous metal–organic framework with high stability for GC separation of alcohols from water, *Chem. Commun.* **2012**, *48*, 7613-7615.

[21] Sun, J. K. ; Ji, M. ; Chen, C. ; Wang, W. G. ; Wang, P. ; Chen, R. P. ; Zhang, J. A charge-polarized porous metal–organic framework for gas chromatographic separation of alcohols from water, *Chem. Commun.* **2013**, *49*, 1624-1626.

[22] Nalaparaju, A. ; Zhaoand, X.S. ; Jiang, J.W. Molecular Understanding for the Adsorption of Water and Alcohols in Hydrophilic and Hydrophobic Zeolitic Metal−Organic Frameworks, *J. Phys. Chem. C* **2010**, *114*, 11542-11550.

[23] Ren, C.-X. ; Ji, M. ; Yao, Q.-X. ; Cai, Q.-X. ; Tan, B. ; Zhang, J. Targeted Functionalization of Porous Materials for Separation of Alcohol/Water Mixtures by Modular Assembly, *Chem. Eur. J.* **2014**, *20*, 14846-14852.

[24] de Lima, G. F. ; Mavrandonakis, A. ; de Abreu, H. A. ; Duarte, H. A. ; Heine, T. Mechanism of Alcohol–Water Separation in Metal–Organic Frameworks, *J. Phys. Chem. C* **2013**, *117*, 4124-4130.

[25] El-Roz, M. ; Thibault-Starzyk, F. ; Blume, A. Infrared study of the silica/silane reaction. *K.G.K.* **2014**, *5*, 53-57.

[26] Surblé, S. ; Serre, C. ; Hong, D.-Y. ; Seo, Y.-K. ; Chang, J.-S. ; Grenèche, J.-M. ; Margiolak, I. ; Férey, G. Synthesis and catalytic properties of MIL-100(Fe), an iron(III) carboxylate with large pores, *Chem. Commun.* **2007**, 2820-2822.

[27] Birsa Čelič, T. ; Rangus, M. ; Lázár, K. ; Kaučič, V. ; Logar, N. Z. Spectroscopic Evidence for the Structure Directing Role of the Solvent in the Synthesis of Two Iron Carboxylates, *Angew. Chem. Int. Ed.* **2012**, *512*, 12490-12494.

[28] Seo, Y.-K.; Yoon, J.W.; Lee, J.S.; Lee, U.-H.; Hwang, Y.K.; Jun, C.-H.; Horcajada, P.; Serre, C.; Chang, J.-S. Large scale fluorine-free synthesis of hierarchically porous iron(III) trimesate MIL-100(Fe) with a zeolite MTN topology, *Microp. Mesop. Mater.* **2012**, *157*, 137-145.

[29] Bazin, P. ; Alenda, A. ; Thibault-Starzyk, F. Interaction of water and ammonium in NaHY zeolite as detected by combined IR and gravimetric analysis (AGIR), *Dalton Trans.* **2010**, *39*, 8432-8436.

[30] Popov, A. ; Kondratieva, E. ; Goupil, J.M. ; Mariey, L. ; Bazin, P. ; Gilson, J.P. ; Travert, A. ; Mauge, F. Bio-oils Hydrodeoxygenation: Adsorption of Phenolic Molecules on Oxidic Catalyst Supports, *J. Phys. Chem. C* **2010**, *114*, 15661-15670.

[31] Moulin, B. ; Oliviero, L. ; Bazin, P. ; Daturi, M. ; Costentin, G. ; Maugé, F. How to determine IR molar absorption coefficients of co-adsorbed species? Application to methanol adsorption for quantification of MgO basic sites, *Phys. Chem. Chem. Phys.* **2011**, *13*, 10797-10807.

[32] Stelmachowski, P. ; Sirotin, S. ; Bazin, P. ; Maugé F. ; Travert, A. Speciation of adsorbed CO2 on metal oxides by a new 2-dimensional approach: 2D infrared inversion spectroscopy (2D IRIS), *Phys. Chem. Chem. Phys.* **2013**, *15*, 9335-9342.

[33] Smith, B. C. «*Infrared Spectral Interpretation: A Systematic Approach* , CRC Press, **1998**.

[34] Jeremias, F. ; Khutia, A. ; Henninger, S. K. ; Janiak, C. MIL-100(Al, Fe) as water adsorbents for heat transformation purposes—a promising application, *J. Mater. Chem.* **2012**, *22*, 10148-10151.

[35] Čelič, T. B.; Mazaj, M.; Guillou, N.; Elkaim, E.; El-Roz, M.; Thibault-Starzyk, F. ; Mali, G.; Rangus, M.; Čendak, T.; Kaucic, V.; Logar, N. Z. Study of Hydrothermal Stability and Water Sorption Characteristics of 3-Dimensional Zn-Based Trimesate, *J. Phys. Chem. C*, **2013**, *117*, 14608-14617.

[36] Baker, E.M. Equilibria in Ethanol-Water System at Pressures Less Than Atmospheric, *Ind. Eng. Chem. Ind. Ed.* **1942**, *34*, 1501-1504.